Journal of Inorganic and Organometallic Polymers and Materials (2018) 28:1432–1438
https://doi.org/10.1007/s10904-018-0802-2

Characterization of Lithium Ion-Conducting Blend Biopolymer Electrolyte Based on CH–MC Doped with $LiBF_4$

Omed Gh. Abdullah[1,2] · Rawad R. Hanna[3] · Yahya A. K. Salman[3] · Shujahadeen B. Aziz[1]

Received: 28 November 2017 / Accepted: 31 January 2018 / Published online: 6 February 2018

Abstract
Lithium ion-conducting polymer blend electrolytes based on chitosan and methylcellulose complexed with lithium tetrafluoroborate ($LiBF_4$) were prepared by a solution-casting method. The features of complexation of the solid polymer electrolytes were studied using X-ray diffraction techniques. Electrical conductivity of the prepared films was measured as a function of frequency at a different temperature. The increased trend of the electrical conductivity with increasing temperature and salt concentration can be attributed to increasing the mobility and number of lithium ions, respectively. The polymer electrolyte system exhibited Arrhenius-type, temperature-dependence ion conductivity behavior. Optical properties such as optical band gap, tail due to localized states and complex refractive index were estimated for present polymer electrolyte system from optical absorption measurement in the wavelength region 190–1100 nm. It was found that the optical direct band gap values shifted to lower energies upon addition of $LiBF_4$ salt up to 40 wt% dopant concentration, and showed an increasing tendency for a further increase in dopant concentration. The high refractive index for this composition (2.44–2.63) at visible wavelengths eminently suitable for optical applications.

Keywords Solid polymer electrolyte · Lithium-ion conducting · Conductivity · High refractive index polymer

1 Introduction

In recent years, studies of optical and electrical properties of solid polymer electrolytes system have received much attention in view of their potential applications in optical and electronic devices such as solid-state rechargeable batteries, electrochromic display devices, fuel cells, super-capacitors, and gas sensors [1–3]. The investigation of electrical conduction in solid polymer electrolyte membrane aimed to understand conduction mechanism and nature of the charge transport predominant in these materials, while the optical characterizations aimed at achieving a high reflection and anti-reflection polarized properties [4, 5]. It is well established in the literature that the optical and electrical properties of polar polymers can be suitably modified by a combination of different inorganic salts [6]. Investigations of solid polymer electrolyte systems have focused primarily on the improvement of ionic conduction of polymer at room temperature [7].

The ionic conductivity of polymer electrolytes is associated with the amorphous phase of materials. Various methods, such as co-polymerization, polymer blending, plasticization, and the addition of nanofillers into polymer materials have been used to improve the ionic conductivity of solid polymer electrolyte systems [8, 9]. Polymer blends have gained commercial importance over homopolymers and copolymers due to low-cost, simplicity of preparation and easy control the physical properties by compositional change; thus polymer blends are most promising and feasible approach to improve the ionic conductivity [10]. In addition, polymer blends often show unique and superior properties not present in the individual polymer components [11, 12]. Researchers have strived to obtain the combination of high ionic conductivity, good thermal, electrochemical and mechanical stability. These improved desirable properties cannot be achieved using single polymer, thus polymer

✉ Omed Gh. Abdullah
omed.abdullah@univsul.edu.iq

[1] Advanced Polymeric Materials Research Lab., Department of Physics, College of Science, University of Sulaimani, Sulaimani, Kurdistan Region 46001, Iraq

[2] Komar Research Center, Komar University of Science and Technology, Sulaimani, Kurdistan Region 46001, Iraq

[3] Department of Physics, College of Science, University of Mosul, Mosul 41002, Iraq

blending is used as one of the most effective methods to improve the required characteristics of solid polymer electrolyte system [13].

Very recently, solid-state electrolyte based on natural polymers (biopolymers or agro-polymers) have drawn the attention of many researchers, as an alternative material for energy storage, due to many advantages such as abundant, water-soluble, non-toxic, environment-friendly, biodegradable, biocompatible, and they have excellent film-forming properties [14–16]. In our previous work, the miscibility between chitosan (CH) and methylcellulose (MC) was investigated, and the optimal blend composition was found to be in ration 75 wt% CH and 25 wt% MC [17].

Although numerous studies have been reported on the investigation of optical and electrical properties of different lithium ion conducting polymer electrolytes [18–20], very little work is available on chitosan–methylcellulose (CH–MC) blend polymer doped with lithium salts. This study presents the results of such investigations on the optical and electrical properties of CH–MC polymer blend films doped with $LiBF_4$. Thus different compositions of CH–MC:$LiBF_4$ polymer blend electrolytes were prepared, and their optimum composition was identified, using structural, electrical, and optical characterizations.

2 Experimental

2.1 Preparation of Solid Polymer Blend Electrolyte

Films of pure polymer blend of CH–MC with 75:25 weight ratio, and various compositions of CH–MC based polymer electrolyte complexed with $LiBF_4$ salt were prepared with different weight percent of the salt (10, 20, 30, 40, and 50 wt%) by a solution casting technique using 2% acetic acid and distilled water as a solvent for CH and MC, respectively. The solutions were stirred for 48 h until the polymer powders are completely dissolved and then cast onto polypropylene Petri dishes and the solvent allowed to evaporate slowly at ambient temperature. The final product was kept in a desiccator filled with silica gel desiccants for further drying. The prepared solid polymer blend electrolyte samples were coded as SPBE0, SPBE10, SPBE20, SPBE30, SPBE40, and SPBE50 for different concentration as described in Table 1.

2.2 Characterization of Solid Polymer Blend Electrolytes

X-ray diffraction (XRD) patterns of the samples were obtained at room temperature using a controlled X'PERT-PRO X-ray diffractometer with Cu–Kα monochromatic radiation of 1.5406 Å wavelengths. Glancing angle (2θ) was varied from 10° to 70° with a step size of 0.1°. The electrical conductivity behavior of a pure and $LiBF_4$ doped CH–MC polymer blend electrolytes was measured using Agilent 4284A Precision LCR Meter in the frequency range 100 Hz–1 MHz and temperature range 295–373 K. The films were fixed on a conductivity holder with two aluminium blocking electrodes (2.5 cm in diameter) under spring pressure. A T-type thermocouple was used to record internal temperature in the chamber with an accuracy of ± 1 °C. Optical absorption spectra of the prepared films were recorded in the wavelength region 190–1100 nm at room temperature using a PerkinElmer Lambda 25 double-beam UV–Vis spectrophotometer. From this data, the optical constants such as optical energy gap, tail of localized state and complex refractive index were determined.

3 Results and Discussion

3.1 XRD Analysis

In order to investigate the modifications in crystal structure of CH–MC polymer blend, upon addition of $LiBF_4$ salt, XRD measurements were performed. Figure 1a–f depicts XRD patterns of CH–MC based polymer blend electrolytes doped with a different concentration of $LiBF_4$ salt. The observed broad peak at $2\theta = 21.1°$ for pure polymer blend films is due to semi-crystalline nature resulting from the intramolecular and intermolecular interaction between polymer chains through hydrogen bonding [21, 22]. The broadening and decreasing in the intensity of this XRD peak with addition of $LiBF_4$ salt denotes the reduction in the degree of

Table 1 Summarizes of composition of CH–MC:$LiBF_4$ solid polymer blend electrolyte films

Designation	CH solution		MC solution		$LiBF_4$ wt%	$LiBF_4$ (g)
	Powder (g)	Solvent (ml)	Powder (g)	Solvent (ml)		
SPBE0	1.50	150	0.50	20	0	0.000
SPBE10	1.50	150	0.50	20	10	0.222
SPBE20	1.50	150	0.50	20	20	0.500
SPBE30	1.50	150	0.50	20	30	0.857
SPBE40	1.50	150	0.50	20	40	1.333
SPBE50	1.50	150	0.50	20	50	2.000

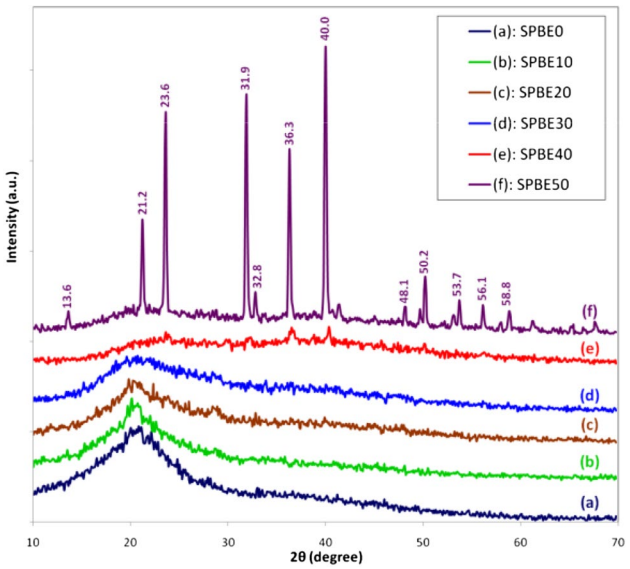

Fig. 1 XRD patterns of blend CH–MC doped with (**a**) 0 wt% $LiBF_4$, (**b**) 10 wt% $LiBF_4$, (**c**) 20 wt% $LiBF_4$, (**d**) 30 wt% $LiBF_4$, (**e**) 40 wt% $LiBF_4$, (**f**) 50 wt% $LiBF_4$

crystallinity of present polymer electrolyte films. The semi-crystalline peak of polymer blend disappeared completely in SPBE40 composite. On the other hand, the absence of sharp diffraction peaks at low $LiBF_4$ salt concentrations indicates that lithium salt was completely dissolved in polymer blend matrix. The amorphous nature results in greater ionic diffusivity with high ionic conductivity [23, 24]. It can be seen clearly that SPBE50 sample shows sharp crystalline peaks at diffraction angle of 13.6°, 21.2°, 23.6°, 31.9°, 32.8°, 36.3°, 40.0°, 48.1°, 50.2°, 53.7°, 56.1° and 58.8°, which attributed to re-crystallization of $LiBF_4$ salt out of the film surface due to recombination of ions at higher salt concentration [25, 26]. The sharp observed peaks in higher salt concentration sample are well matched with the standard data from JCPDS card number 40-0664.

3.2 Ionic Conductivity

The variation of direct-current (dc) conductivity (σ_{dc}) as a function of temperature for CH–MC blend films at different weight percent ratios of $LiBF_4$ is tabulated in Table 2. The room temperature σ_{dc} for pure polymer blend sample was found to be 5.3×10^{-8} S cm^{-1}. It increased with increasing lithium salt concentration up to 40 wt% to reach 3.747×10^{-6} S cm^{-1}, however, it decrease for 50 wt% $LiBF_4$ contents. Therefore, 40 wt% $LiBF_4$ salt is the conductivity optimizing concentration. In general, the conductivity of polymer electrolyte materials can be described by the relationship:

$$\sigma = \sum q_i n_i \mu_i \quad (1)$$

where q_i, n_i and μ_i represent the charge, concentration and mobility of the i species, respectively [27]. Hence, the increase in the conductivity with increasing $LiBF_4$ concentrations could be attributed to the increase in the number density of mobile ions (charge-carriers), as well as the enhancement in the charge-carrier mobility due to improvement of amorphous nature of the host polymer blend as confirmed previously by XRD studies (see Fig. 1e). The decrease in conductivity at higher salt concentrations (50 wt%) is due to inability of the salt to be accommodated by the polymer host resulted in recombination of the ions and recrystallization of lithium salt out of the polymer film surface [28]. This phenomenon impedes the conduction process. This result was supported by XRD analysis, which clearly shows formation of $LiBF_4$ salt crystal on the surface of the high salt concentration polymer electrolyte sample (Fig. 1f). Similar behavior was also observed in a number of polymer electrolyte films [26, 28, 29].

Comparison between these results and previously reported measures; It is worth mentioning that the maximum conductivity at ambient temperature obtained in this study is higher than that obtained by Tang et al. [30] (4.39×10^{-7} S cm^{-1}) for $LiBF_4$ complexed PVdF-HFP polymer electrolyte films.

It is interesting to note that the electrical conductivity increased with increasing temperature and followed Arrhenius equation in the investigated temperature region. In solid polymer electrolyte films, the change in electrical conductivity with temperature is highly related to the segmental chain motion, which results to increase in free

Table 2 Temperature-dependent dc conductivity (σ_{dc}) for CH–MC:$LiBF_4$ polymer blend electrolyte

Samples	$\sigma_{dc} \times 10^{-6}$ (S cm^{-1}) at different temperatures								
	295 K	303 K	313 K	323 K	333 K	343 K	353 K	363 K	373 K
SPBE0	0.053	0.105	0.304	0.754	1.931	4.249	9.523	22.383	37.921
SPBE10	0.145	0.334	0.878	2.431	6.086	13.476	28.000	54.592	92.485
SPBE20	0.394	0.883	2.520	6.720	15.52	33.199	60.198	128.832	219.391
SPBE30	1.154	2.555	6.405	15.982	42.174	86.591	152.439	300.321	502.794
SPBE40	3.747	7.828	20.388	48.299	113.217	217.477	411.128	768.736	1426.413
SPBE50	1.412	2.738	8.465	19.035	46.334	79.257	170.613	338.338	604.938

volume of the host polymer [31, 32]. As the temperature is increased, the molecular segments gain more vibrational energy and create a small amount of free volume around polymer chain causes an increase in mobility of ions and polymer segments and, hence, the conductivity [33, 34]. Similar behavior was also observed in many other solid polymer electrolyte films [5, 35, 36]. As per the Arrhenius equation, temperature-dependence electrical conductivity has the form:

$$\sigma = \sigma_o \exp\left(-E_a/k_B T\right) \tag{2}$$

where σ_o is proportionality constant, E_a is activation energy, k_B is Boltzmann constant and T is absolute temperature. The value of activation energies (E_a) were estimated with the help of the slopes of $\log(\sigma)$ versus $1000/T$ plots shown in Fig. 2. The E_a value for pure CH–MC polymer blend film was found to be 0.815 eV, this value was reduced to 0.798, 0.773, 0.749, 0.722 and 0.740 eV for SPBE10, SPBE20, SPBE30, SPBE40 and SPBE50, respectively. It is clear that the activation energy of conductivity tends to decrease with increasing lithium salt concentration up to 40 wt% $LiBF_4$ which have the maximum conductivity at all temperature (see Table 2). The increase in electrical conductivity and decrease in activation energy values for the present polymer electrolyte systems can be explained on the basis that the addition of lithium salt forms charge-transfer complexes in host lattice [30]. These charge transfer complexes increase the electrical conductivity by providing additional mobile charge carriers in the lattice, which lead to decrease in the activation energy [37]. Similar observations were also reported by number of research teams for different polymer electrolytes. Buraidah and Arof [38] reported that the highest conducting sample in the chitosan/PVA blend electrolyte doped with NH_4I system has the lowest activation energy.

3.3 Optical Absorption Studies

The study of optical absorption spectra provides useful information about the electronic band structure of solids. Electronic transitions in insulator and semiconductor materials can be generally classified into two categories; (i) direct and (ii) indirect band gap. In direct band gap transitions, the top of the valence band and the bottom of conduction band both lie at the same value of wave vector (zero crystal momentum). If the top of the valence band and the bottom of conduction band lie in different wave vector (does not correspond to zero crystal momentum), it is termed as an indirect band gap transitions [39, 40].

Optical absorption measurements on CH–MC:$LiFB_4$ polymer blend electrolyte films were carried out to determine the optical properties like; optical band gap, tail of localized state and complex refractive index. The absorption coefficient was determined from absorbance (A) spectra using the formula [41]:

$$\alpha = 2.303\left(\frac{A}{d}\right) \tag{3}$$

where d is thickness of the film.

The UV–Vis absorption coefficient spectra of prepared CH–MC:$LiBF_4$ polymer electrolyte films with different salt concentration are depicted in Fig. 3. The value of absorption depends upon radiation energy as well as composition of the film. The appearance of two broad absorption peaks at 268 and 345 nm for both pure and doped CH–MC blend polymer electrolyte films are assigned to $\pi \rightarrow \pi^*$ and $n \rightarrow \pi^*$electronic transitions, respectively.

For the direct band gap transitions, the absorption coefficient dependence on the incident photon energy (hv) as following [42, 43]:

$$\alpha hv = \beta\left(hv - E_g\right)^{1/2} \tag{4}$$

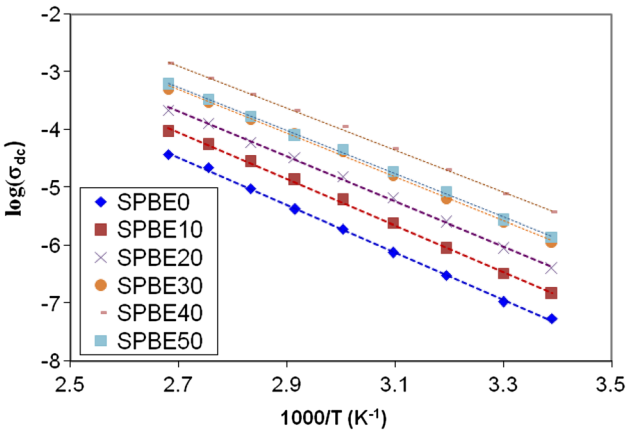

Fig. 2 Variation of $\log\left(\sigma_{dc}\right)$ versus $1000/T$ for CH–MC:$LiBF_4$ solid polymer blend electrolyte films

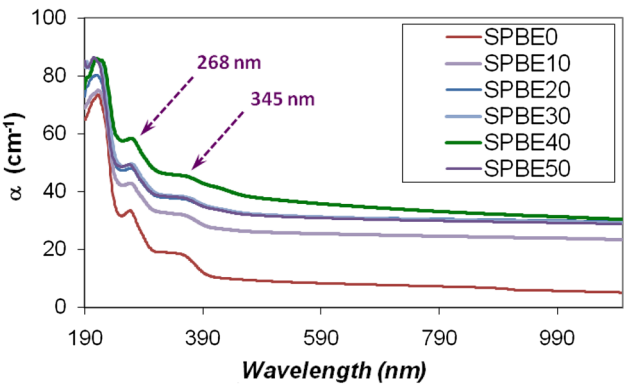

Fig. 3 Absorbance coefficient spectra for CH–MC:$LiBF_4$ solid polymer electrolyte system

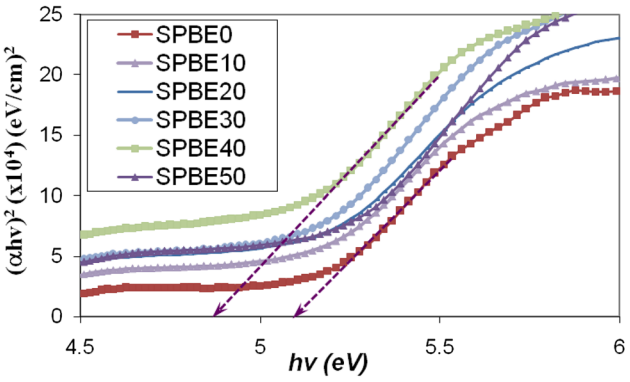

Fig. 4 Variation of $(\alpha hv)^2$ versus (hv) for CH–MC:$LiBF_4$ solid polymer blend electrolyte films

where E_g is optical band gap energy, β is a structure-dependent constant, h is Planck's constant, and v is frequency of the incident light.

Figure 4 depicted the variation of $(\alpha hv)^2$ versus (hv) for different components of CH–MC:$LiBF_4$ polymer electrolyte films. The allowed direct transition energies were determined by extrapolating the linear region of each curve to zero absorption. For pure CH–MC polymer film the direct band gap found to be 5.10 eV, this value was slightly reduced to 5.03, 5.02, 4.98, and 4.88 eV for 10, 20, 30 and 40 wt% $LiBF_4$ doped CH–MC polymer electrolyte, respectively. It is interesting to note that the optical band gap was increased again to 5.04 eV for 50 wt% $LiBF_4$ salt content.

Thus, the direct band gap energy shows a decreasing trend upon addition of $LiBF_4$ salt up to a dopant concentration of 40 wt%. For a further increase in lithium salt concentration, these values started increasing. The similar behavior was also observed for electrical activation energies calculated from temperature-dependent electrical conductivity data shown in Fig. 2. However, the magnitudes of the calculated electrical activation energies are smaller in comparison with the optical band gap energies. This is because of truth that their nature is different. While optical band gap corresponds to electron inter-band transitions, the activation energy corresponds to the energy required for conduction from one site to another [44, 45].

The reduction in the optical band gap of the present polymer electrolyte films with increasing $LiBF_4$ content, could be ascribed to the formation of a new energy levels in the forbidden band gap, due to increase in amorphous fraction of CH–MC polymer blend, which facilitate the transmission of electrons from the top of valence band to the bottom of the conduction band through these new localized states [46, 47], consequently the band gap decreases with increasing $LiBF_4$ content. In other words, the increase in the amorphous fraction results in a decrease in the optical band gap of the films.

To understand the amorphous feature further, the width of band tail due to localized state of the present polymer electrolyte films were calculated from UV–Vis absorption spectra according to Urbach rule:

$$\alpha = \alpha_o \exp\left(hv/E_U\right) \tag{5}$$

where α_o is a constant and E_U is Urbach energy represent the width of tail localized states in the forbidden band [48, 49]. Figure 5 depicts the logarithmic variation of absorption coefficient ln (α) versus incident photon energy (hv). The value of E_U were calculated by taking the reciprocals of the slopes of linear portion of Fig. 5. The calculated values of E_U are 1.270, 1.795, 1.798, 1.926, 2.551 and 1.345 eV for samples SPBE0, SPBE10, SPBE20, SPBE30, SPBE40 and SPBE50, respectively. Usually the value of E_U represents the defects present within the materials, thus, the maximum E_U value for SPBE40 suggests the maximum defect fraction, and hence the minimum E_g [50]. This result was supported by XRD analysis, and compatible with the obtained results from Fig. 4.

3.4 Complex Refractive Index

The complex refractive index is an essential parameter in design and fabrication of advanced optical and optoelectronic devices. For further understand the interaction of lithium ions with CH–MC blend polymer matrix, the value of refractive index was calculated from fundamental optical relationship by using reflectance (R) and extinction coefficient (k) of films [51]:

$$n = \sqrt{\frac{4R}{(1-R)^2} - k^2} - \frac{R+1}{R-1} \tag{6}$$

where $k = \lambda\alpha/4\pi$, and the reflectance (R) was determined from absorption (A) and transmittance (T) spectra data by using the relationship $R = 1 - (A + T)$, [52].

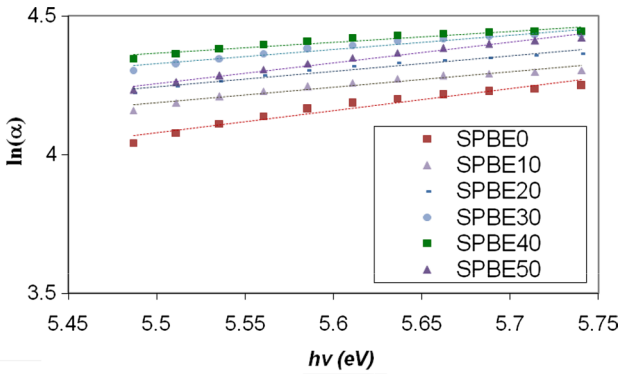

Fig. 5 Variation of ln (α) versus (hv) for different component of CH–MC:$LiBF_4$ solid polymer electrolyte films

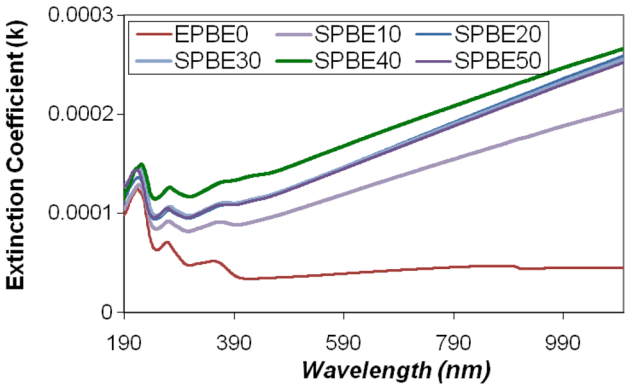

Fig. 6 Extinction coefficient (k) spectra for CH–MC:$LiBF_4$ solid polymer blend electrolyte films

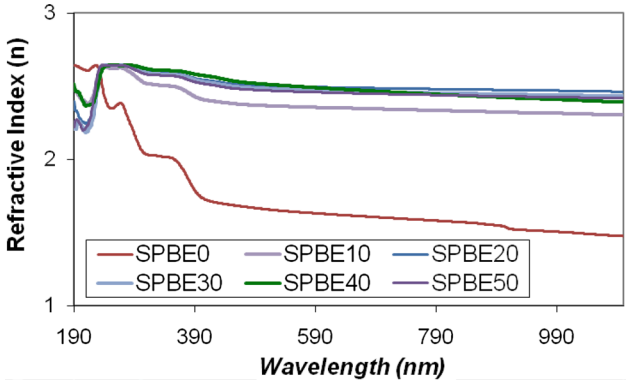

Fig. 7 Refractive index (n) spectra for CH–MC:$LiBF_4$ solid polymer blend electrolyte films

Figures 6 and 7 show the extinction coefficient (k) and the refractive index (n) distributions of CH–MC:$LiBF_4$ solid polymer blend electrolyte films. It is obvious from Fig. 6, that k value of all electrolyte films show an increase with increasing the wavelength of the incident photons from 300 up to 1100 nm.

It can be discerned from Figs. 6 and 7 that the extinction coefficient (k) and the refractive index (n) of solid polymer electrolyte films is higher than that of pure polymer blend and it increases with increasing lithium salt concentration, and shows a maximum values at 40 wt% salt content. The physical properties of materials are considerably reliant on the internal structure of the substances, such as packing density and molecular-weight distributions. The addition of $LiBF_4$ salt to CH–MC polymer blend system, cause an increase in the degree of disorder which may increase the mobility of polymer segments as well the free radicals which are chemically active and cause the formation of localized electronic state. As a result, an increase in the refractive index is obtained [53, 54]. The high refractive index of present solid polymer electrolyte films (2.44–2.63) at visible wavelengths indicated that these films could be used in optoelectronic devices [55, 56].

4 Conclusions

These studies indicate that CH–MC blend polymer can be effectively doped with $LiBF_4$ to enhance its electrical and optical behaviors. Maximum room temperature conductivity has been obtained for a sample containing 40 wt% $LiBF_4$. This enhancement has been explained on the basis of charge transfer complex formation, as well as the improvement in the amorphous fraction of polymer electrolyte samples. The increase in salt concentration beyond 40 wt% resulted in a decrease in conductivity owing to recombination of ions at higher salt concentrations. Optical absorption studies showed a decreasing trend of the optical band gap with increased salt concentration up to 40 wt%. For a further increase in salt concentration, these values started increasing again due to recombination of the ions and recrystallization of the salt out of the film surface. These results point to the fact that 40 wt% of $LiBF_4$ content is the critical concentration that gives optimum values for the electrical and optical properties.

Acknowledgements The authors gratefully acknowledge the Ministry of Higher Education and Scientific Research, University of Sulaimani, and the Komar University of Science and Technology, for the facility in their laboratories and the financial support given to this work.

Compliance with Ethical Standards

Conflict of interest The authors declare no conflict of interest.

References

1. A.F. Abdulameer, M.H. Suhail, O.G. Abdullah, I.M. Al-Essa, J. Mater. Sci. Mater. Electron. **28**, 13472–13477 (2017)
2. M.H. Suhail, A.A. Ramadan, S.B. Aziz, O.G. Abdullah, J. Sci. Adv. Mater. Device. **2**, 301–308 (2017)
3. K. Ramly, M.I.N. Isa, A.S.A. Khiar, Mater. Res. Innov. **15**, S82-85 (2011)
4. O.G. Abdullah, A.K. Yahya, S.A. Salman, Phys. Mater. Chem. **3**, 18–24 (2015)
5. V.B.S. Achari, T.J.R. Reddy, A.K. Sharma, V.V.R.N. Rao, Ionics. **13**, 349–354 (2007)
6. O.G. Abdullah, S.B. Aziz, K.M. Omer, Y.M. Salih, J. Mater. Sci. Mater. Electron. **26**, 5303–5309 (2015)
7. K.R. Mohan, V.B.S. Achari, V.V.R.N. Rao, A.K. Sharma, Polym. Test. **30**, 881–886 (2011)
8. S.F. Bdewi, O.G. Abdullah, B.K. Aziz, A.A.R. Mutar, J. Inorg. Organomet. Polym. Mater. **26**, 326–334 (2016)
9. O.G. Abdullah, S.B. Aziz, M.A. Rasheed, Ionics. (2017). https://doi.org/10.1007/s11581-017-2228-1
10. R.T. Abdulwahid, O.G. Abdullah, S.B. Aziz, S.A. Hussein, F.F. Muhammad, M.Y. Yahya, J. Mater. Sci. Mater. Electron. **27**, 12112–12118 (2016)

11. K. Ramamohan, V.B.S. Achari, A.K. Sharma, L. Xiuyang, Ionics. **21**, 1333–1340 (2015)
12. F.F. Hatta, M.Z.A. Yahya, A.M.M. Ali, R.H.Y. Subban, M.K. Harun, A.A. Mohamad, Ionics. **11**, 418–422 (2005)
13. Y. Yang, T. Inoue, T. Fujinami, M.A. Mehta, Solid State Ionics. **140**, 353–359 (2001)
14. N.A.N. Aziz, N.K. Idris, M.I.N. Isa, Int. J. Polym. Anal. Charact. **15**, 319–327 (2010)
15. A.M.M. Gomes, P.L. Silva, C.L. Moura, C.E.M. Silva, N.M.P.S. Ricardo, Macromol. Symp. **299/300**, 220–226 (2011)
16. K.C. Basavaraju, T. Damappa, S.K. Rai, Carbohyd. Polym. **66**, 357–362 (2006)
17. O.G. Abdullah, R.R. Hanna, Y.A.K. Salman, J. Mater. Sci. Mater. Electron. **28**, 10283–10294 (2017)
18. A.M. Stephan, K.S. Nahm, Polymer. **47**, 5952–5964 (2006)
19. R. Malini, U. Uma, T. Sheela, M. Ganesan, N.G. Renganathan, Ionics. **15**, 301–307 (2009)
20. S.Z. Yusof, H.J. Woo, A.K. Arof, Ionics. **22**, 2113–2121 (2016)
21. O.G. Abdullah, S.A. Saleem, J. Electron. Mater. **45**, 5910–5920 (2016)
22. M. Hasegawa, A. Isogai, F. Onabe, M. Usuda, R.H. Atalla, J. Appl. Polym. Sci. **45**, 1873–1879 (1992)
23. S. Rajendran, T. Mahalingam, R. Kannan, Solid State Ionics. **130**, 143–148 (2000)
24. O.G. Abdullah, S.B. Aziz, D.R. Saber, R.M. Abdullah, R.R. Hanna, S.R. Saeed, J. Mater. Sci. Mater. Electron. **28**, 8928–8936 (2017)
25. M.F. Shukur, M.F.Z. Kadir, Electrochim. Acta. **158**, 152–165 (2015)
26. S.B. Aziz, O.G. Abdullah, M.A. Rasheed, H.M. Ahmed, Polymers. **9**, 187 (2017)
27. Z. Osman, M.I.M. Ghazali, L. Othman, K.B.M. Isa, Results Phys. **2**, 1–4 (2012)
28. M.F.Z. Kadir, S.R. Majid, A.K. Arof, Electrochim. Acta. **55**, 1475–1482 (2010)
29. M.M. Noor, M.A. Careem, S.R. Majid, A.K. Arof, Mater. Res. Innov. **15**, S2-157 (2011)
30. J. Tang, R. Muchakayala, S. Song, M. Wang, K.N. Kumar, Polym. Test. **50**, 247–254 (2016)
31. S. Rajendran, M. Sivakumar, R. Subadevi, Mater. Lett. **58**, 641–649 (2004)
32. O.G. Abdullah, Y.A.K. Salman, S.A. Saleem, J. Mater. Sci. Mater. Electron. **27**, 3591–3598 (2016)
33. R. Baskaran, S. Selvasekarapandian, G. Hirankumar, M.S. Bhuvaneswari, Ionics. **10**, 129–134 (2004)
34. C.H. Park, D.W. Kim, J. Prakash, Y.K. Sun, Solid State Ionics. **159**, 111–119 (2003)
35. N. Reddeppa, T.J.R. Reddy, V.B.S. Achari, V.V.R.N. Rao, A.K. Sharma, Ionics. **15**, 255–259 (2009)
36. T.J.R. Reddy, V.B.S. Achari, A.K. Sharma, V.V.R.N. Rao, Ionics. **13**, 435–439 (2007)
37. A.S.A. Khiar, A.K. Arof, Ionics. **16**, 123–129 (2010)
38. M.H. Buraidah, A.K. Arof, J. Non-Cryst. Solids. **357**, 3261–3266 (2011)
39. S.B. Aziz, O.G. Abdullah, S.A. Hussein, H.M. Ahmed, Polymers. **9**, 622 (2017)
40. S.B. Aziz, O.G. Abdullah, M.A. Rasheed, J. Mater. Sci. Mater. Electron. **28**, 12873–12884 (2017)
41. S.B. Aziz, O.G. Abdullah, M.A. Rasheed, J. Appl. Polym. Sci. **134**(1–8), 44847 (2017)
42. O.G. Abdullah, S.B. Aziz, M.A. Rasheed, J. Mater. Sci. Mater. Electron. **28**, 4513–4520 (2017)
43. L.I. Buruiana, E. Avram, A. Popa, V.E. Musteata, S. Ioan, Polym. Bull. **68**, 1641–1661 (2012)
44. O.G. Abdullah, S.B. Aziz, M.A. Rasheed, Results Phys. **6**, 1103–1108 (2016)
45. C. Umadevi, A.K. Sharma, V.V.R.N. Rao, J. Mater. Lett. **56**, 167–174 (2002)
46. O.G. Abdullah, J. Mater. Sci. Mater. Electron. **27**, 12106–12111 (2016)
47. V. Krishnakumar, G. Shanmugam, Ionics. **18**, 403–411 (2012)
48. S.D. Praveena, V. Ravindrachary, R.F. Bhajantri, Ismayil, Polym. Compos. **27**, 987–997 (2014)
49. O.G. Abdullah, D.A. Tahir, K. Kadir, J. Mater. Sci. Mater. Electron. **26**, 6939–6944 (2015)
50. R.P. Chahal, S. Mahendia, A.K. Tomar, S. Kumar, J. Alloy. Compd. **538**, 212–219 (2012)
51. S.B. Aziz, M.A. Rasheed, S.R. Saeed, O.G. Abdullah, Int. J. Electrochem. Sci. **12**, 3263–3274 (2017)
52. S. Agarwal, V.K. Saraswat, Opt. Mater. **42**, 335–339 (2015)
53. A.M. El Sayed, H.M. Diab, R. El-Mallawany, J. Polym. Res. **20**(1–10), 255 (2013)
54. I. Saini, J. Rozra, N. Chandak, S. Aggarwal, P.K. Sharma, A. Sharma, Mater. Chem. Phys. **139**, 802–810 (2013)
55. S. Sugumaran, C.S. Bellan, Optik. **125**, 5128–5133 (2014)
56. T. Higashihara, M. Ueda, Macromolecules. **48**, 1915–1929 (2015)